IEEE Access
Multidisciplinary | Rapid Review | Open Access Journal

Received 27 October 2023, accepted 15 November 2023, date of publication 16 November 2023,
date of current version 21 November 2023.

Digital Object Identifier 10.1109/ACCESS.2023.3334162

RESEARCH ARTICLE

Investigating the Effect of Handover on Latency in Early 5G NR Deployments for C-V2X Network Planning

JOSEPH CLANCY[1,2], DARRAGH MULLINS[1,2], ENDA WARD[3], PATRICK DENNY[4], (Member, IEEE), EDWARD JONES[1,2], (Senior Member, IEEE), MARTIN GLAVIN[1,2], (Member, IEEE), AND BRIAN DEEGAN[1,2]

[1]Department of Electrical and Electronic Engineering, University of Galway, Galway, H91 TK33 Ireland
[2]Ryan Institute, University of Galway, Galway, H91 TK33 Ireland
[3]Valeo, Tuam, Galway, H54 Y276 Ireland
[4]Department of Electronic and Computer Engineering, University of Limerick, Limerick, V94 T9PX Ireland

Corresponding author: Joseph Clancy (J.CLANCY6@nuigalway.ie)

This work was supported in part by the Connaught Automotive Research (CAR) Group, University of Galway; and in part by the Science Foundation Ireland co-funded under the European Regional Development Fund through the Southern & Eastern Regional Operational Programme to Lero—The Science Foundation Ireland Research Centre for Software (www.lero.ie) under Grant 13/RC/2094_P2.

ABSTRACT Vehicle-to-Everything (V2X) communication technology aims to enhance intelligent vehicles' coordination and perception by enabling interactions with other vehicles, road users, and infrastructure. Although 4th and 5th generation cellular technologies (4G LTE and 5G NR) can support non-safety V2X communication, their design, rooted in multimedia and telephony, doesn't align well with safety-critical applications. Despite the advancements of 5G NR over 4G LTE, ensuring reliable Quality-of-Service (QoS) metrics remains a notable concern. The process of handover, a core cellular network function, significantly contributes to the challenges in cellular communication reliability. To assess handover's impact on latency in V2X communication scenarios, a driving-focused measurement campaign was executed on an early 5G NR-enabled commercial cellular network. Findings reveal that, in terms of its effect on end-user latency, the more mature 4G LTE network displays on average 63% (intra-freq.) and 36% (inter-freq.) lower latency costs when performing handovers compared to early 5G NR deployments. Notably, inter-generation handovers (4G to 5G and vice versa) exhibit 24% (intra-freq.) and 10% (inter-freq.) higher average latency costs with respect to other handover types. Furthermore, discernible variations in network reliability emerge between distinct V2X scenarios such as urban and rural environments. The prevailing reliability concerns tied to present handover algorithms hold substantial weight, as they undermine intelligent vehicles' trust in network-received information. Consequently, these outcomes underscore the urgency for designing and implementing handover strategies better suited to the dynamic mobility characteristics of intelligent vehicles across diverse V2X scenarios.

INDEX TERMS V2X, V2X communications, vehicle-to-everything, vehicular networks, intelligent transport systems, ITS, cellular, C-V2X, 4G LTE, 5G NR, handover, latency, network planning.

I. INTRODUCTION

In recent years, the intelligent vehicle concept and the industry of Intelligent Transport Systems (ITS) have become technologically and commercially feasible. This is highlighted by the ongoing research and commercial deployments from automotive companies such as Cruise [1], Alphabet's Waymo [2], Tesla [3] and Uber [4]. As a result of these developments, there is increased research and industry interest in what is known as the *connected* intelligent vehicle. Also known as Vehicle-to-Everything (V2X) communications, the concept of the connected intelligent vehicle is a natural extension of existing efforts to integrate advanced sensing and computation capabilities into a vehicle. As a consequence, substantial amounts of data are being generated and processed by the intelligent vehicles, as such this data could be

The associate editor coordinating the review of this manuscript and approving it for publication was Ronald Chang.

offloaded from the vehicle to other parties of interest such as other nearby vehicles or traffic management authorities. This particular interest in V2X communications is highlighted by activities undertaken by wireless communications standards organisations such as the 3GPP [5], [6] for cellular and the IEEE [7] for Wi-Fi.

In general, the term V2X communications describes a system that would allow connected intelligent vehicles to exchange information with other road users or relevant stakeholders. Thus, the primary aim of a V2X communications system is to increase road safety and traffic efficiency by enabling stakeholders in a road traffic environment to communicate and therefore coordinate with one other. A large catalogue of use cases and applications arise from the introduction of V2X communications that concern not only safety and traffic efficiency but also infotainment and eCommerce applications [8]. Consequentially, these potential use cases and applications can involve a non-trivial number and variance of stakeholders, and as such require a robust, secure and reliable underlying wireless communications technology.

Cellular communications, developed by the 3GPP [9], has been considered as a candidate technology for V2X communications for many years [10]. Cellular communications is commonly referred to as C-V2X (Cellular-V2X) in the context of V2X communications. This interest in cellular as a potential V2X access technology is largely due to the existing widespread base station deployments available globally, which would enable C-V2X to serve various end-user types i.e., vehicles, trains, pedestrians and static infrastructures. Several specifications for C-V2X were developed by the 3GPP, the first of which was developed as part of 3GPP Release 14 [11] in 2017, often known as LTE-V2X, and another was developed as part of the introduction of the 5th generation of cellular (5G NR) in 3GPP Release 15 [12] in 2019, often known as NR-V2X.

Previous studies [13], [14], [15], [16] have demonstrated that C-V2X can reliably maintain Quality of Service (QoS) metrics required to support basic non-safety V2X applications outlined by the 3GPP [8]. However, as is the motivation of this work, significant issues still remain surrounding reliability and stability and as such C-V2X cannot reliably support advanced safety-critical use cases. The service requirements developed for 5G NR [17] indicate significant promise for C-V2X to be able to provide the reliability required for advanced safety V2X applications. Handover plays a crucial role in the cellular network, ensuring the degree of QoS that C-V2X can maintain. Effectively managing the movement of participants connected to the C-V2X network is vital for the success of V2X applications. This is because different users within the V2X network have distinct mobility characteristics and patterns. For instance, vehicles generally move at higher speeds compared to pedestrians, yet pedestrians can change their direction more quickly than vehicles.

The aim of this work is to expand on the results and findings presented in [16] to provide a deeper understanding of the effects of handover on end-user latency performance in V2X communications scenarios. Latency is often considered the key metric to enabling safety-critical real-time applications. In the context of V2X communications, this consideration is particularly pertinent due to the risk of the intelligent vehicle making a misinformed decision based on delayed or outdated information about its environment. Unlike similar works that study the effect of handover on network Key Performance Indicators (KPIs), the commercial network under study in this work features early 5G NR deployments. In addition, an analysis of different automotive scenarios is also provided for further insight into key considerations for V2X applications. Results and findings presented here can be used by Mobile Network Operators (MNOs) to inform the planning and implementation of future 5G NR deployments with the aim of increasing the cellular network's capability to support V2X applications and use cases.

The remainder of this paper is structured as follows, in Section II the related work is revised. Section III presents an overview of handover mechanisms in 4G LTE and 5G NR. Section IV outlines the experimental methodology used to conduct measurements and Section V discusses the data processing and analysis methods used in this work. Section VI presents the results of the analysis, discusses the effects of handover and proposes methods to address them. Section VII discusses the limitations of this study and future work. Finally, Section VIII concludes this paper.

II. RELATED WORK

Evaluating the effect of handover on network KPIs is well-studied in the cellular communications literature. However, there are significantly fewer studies evaluating the effect of handover on network KPIs in V2X scenarios. Moreover, there are even fewer driving-based studies evaluating either commercial or private cellular networks as opposed to those that utilise theoretical analysis or simulation. Typically, in the context of V2X communications works typically provide survey or tutorial content on handover mechanisms in cellular networks, evaluations of the performance of handovers in the cellular network or presentations of handover algorithms, particularly for 5G NR.

For the benefit of the reader, a small number of tutorial/survey works are briefly discussed for further context and learning. Tayyab et al. [18] provide a robust tutorial survey of the transitions in handover management from 4G LTE to 5G NR. As part of their survey, Tayyab et al. present a thorough overview of the prevailing challenges in current handover strategies. A challenge of particular note is that of high mobility and the authors discuss a number of solutions around cell deployment strategies. Gures et al. [19] follow on from the previous work and deliver a very comprehensive tutorial on 5G NR-based handover management with a particular focus on the mmWave frequency range introduced with 5G

NR. Gures et al. also provide an in-depth discussion on the beam management issues surrounding utilising these mmWave frequencies to serve devices with high mobility. Lastly, Alraih et al. [20] provide a broad survey on handover or mobility management in what authors describe as Beyond 5G (B5G) or 6G networks. Alraih et al. discuss at length the stringent requirements imposed for 6G networks and the technologies and techniques that will play a role in enabling them.

As is highlighted by the tutorial/survey studies cited above, existing handover techniques are designed and optimised towards mobile handsets which have different mobility characteristics to cellular-enabled vehicles, as such existing handover strategies suffer in high mobility scenarios. This challenge surrounding high mobility scenarios is further highlighted by many authors [21], [22], [23]. Sultan et al. [23] in particular demonstrate this in their comparison between a cellular network consisting only of large (macro) cells and a cellular network composed of many cell sizes (macro, micro, pico). Handover between cells (inter-/intra-frequency) and between radio access technologies (RATs) i.e., 2G, 3G, 4G, 5G has been shown to have a significant effect on network performance [14], [15], [24], [25], [26]. Neumueier et al. [15] report that handovers between cellular generations have the largest impact on latency performance.

Regions with several MNOs offering different coverage capabilities also present a significant concern [14], [25], [27], [28]. Notably, Sliwa et al. [25] and Fernandez et al. [28] demonstrate, via proposed solutions in the form of shared infrastructure, that for cellular to succeed as a V2X communications solution, inter-MNO or inter-PLMN (Public Land Mobile Network) handover is also a key challenge that requires consideration.

The handover algorithms or strategies that result in these observed effects on network KPIs are the subject of quite an active area of communications research. In general, improvements proposed or introduced aim to tackle two key issues in the handover procedure in cellular communications: handover failures and user data interrupt time [18], [29]. These metrics represent the reliability and latency performance of the handover procedure, and both require careful consideration, particularly for V2X communications.

As highlighted by Tayyab et al. [18], existing handover strategies based on a break-before-make or hard handover procedure cannot guarantee handover success or low interrupt time in challenging radio channel scenarios. As such, a modification of the existing handover procedure known as Conditional Handover (CHO) [30], was introduced as part of 3GPP Release 16 [5] in 2020, to guarantee handover success and low interrupt time. A version of this modification was proposed by Park et al. [29] two years prior. Since this time, CHO has gained significant interest in the field of handover with modifications and adjustments being proposed to improve on Radio Link Failures (RLFs) [31] and to minimise signalling overhead [32], [33].

As a result of this adoption of the CHO algorithm to address handover failures and handover interrupt time, several works now focus on the decision-making aspect of CHO i.e., when an early handover command should be executed. As such, a number of prediction algorithms and strategies for the early handover decision process have been proposed. Zhao et al. [34] propose a Recursive Least Squares (RLS) algorithm that leverages multi-connectivity for handover decisions. Several deep learning-based approaches are proposed by several works [35], [36], [37], [38]. Qi et al. [37] in particular propose a predictive handover algorithm alongside a resource reservation mechanism which works in tandem to uphold network QoS metrics. Das et al. [39] provide an interesting prediction algorithm based on Doppler shifts to provide a prediction mechanism similar to that provided by Zhao et al. [34]. Other notable prediction algorithms include a combined graph theory and Reinforcement Learning (RL) approach [40] and an approach based on plant propagation [41] which provide robust results compared to standard so-called reactive handover strategies.

III. OVERVIEW OF HANDOVER IN CELLULAR COMMUNICATIONS

In the following section, an overview of the most relevant concepts surrounding handover in cellular communications is presented. In general, handover will occur as a result of two necessary functions of the cellular network: mobility management and congestion control. As an example, the former occurs as a result of poor channel conditions as a cellular device (a.k.a user equipment or UE) travels towards the edge of a cell, reducing the serving base station's (S-BS) ability to uphold Quality-of-Service (QoS) metrics. Thus, the cellular device, with the aid or direction of the S-BS must transfer to a target base station (T-BS) with more favourable channel conditions. The latter occurs as a result of the S-BS becoming congested due to a large number of devices requiring access to the cellular network. In this scenario, the S-BS will request the offloading of some of its users to another T-BS with similar channel conditions and QoS capabilities.

A. HANDOVER TYPES

The cellular network employs different types of handovers for mobility management or congestion control, depending on the particular domain or layer of the network where they need to take place. Consequently, the level of control signalling needed for each successive handover type varies based on the cellular network entities that are involved. Below is an overview of these handover types, listed from the least to the most control signalling required, although the list is not exhaustive.

- **Intra-/Inter-Frequency:** An S-BS and a T-BS are referred to as intra-frequency neighbours if they operate on the same carrier frequency. Conversely, if an S-BS and T-BS operate on different carrier frequencies, they are referred to as inter-frequency neighbours. The

measurements performed by a UE will differ depending on whether or not the S-BS and T-BS are intra-frequency or inter-frequency neighbours.

- **Intra-/Inter-Cell Layer** A common technique to remedy congestion issues or gaps in a cellular network's coverage is that of heterogeneous networks (HetNets). HetNets involve deploying cells of different sizes, typically referred to as macro, micro and pico cells, often with smaller cells deployed within larger cells. When an S-BS and a T-BS are of the same size i.e., macro-macro, they are referred to as inter-layer neighbours. Conversely, if the S-BS and T-BS are of different sizes i.e., macro-pico they are referred to as inter-layer neighbours.
- **Intra-/Inter-RAT** Each of the cellular generations typically introduces a portion of their technological improvement via different wireless access technologies or RATs. As such, when an S-BS and T-BS share the same RAT they are known as intra-RAT neighbours. Conversely, if the S-BS and T-BS operate on different RATs they are known as inter-RAT neighbours. Inter-RAT handovers typically occur for congestion control or due to deployment limitations.
- **Intra-/Inter-eNodeB/gNodeB** A more recent form on handover introduced as part of 4G LTE is that between eNobdeB (4G LTE) or gNodeB (5G NR). These network entities are used to manage one or more cell sectors or cell sites. If the S-BS and T-BS belong to the same eNodeB/gNodeB then they are referred to as intra-eNodeB or intra-gNodeB neighbours. Conversely, if the S-BS and T-BS do not belong to the same eNodeB/gNodeB they are referred to as inter-eNodeB/inter-gNodeB neighbours.
- **Intra-/Inter-MME/AMF** Alongside the introduction of the eNodeB/gNodeB type handover, another type of handover applies to the Mobility Management Entity (MME - 4G LTE) or the Access and Mobility Management Function (AMF - 5G NR). These core network entities manage UEs in their access of and mobility within the cellular network. Likewise with the eNodeB/gNodeB handover type, if an S-BS and T-BS belong to the same MME/AMF they are known as intra-MME/AMF neighbours. Conversely, for cellular networks of significant size, an S-BS and T-BS being managed by different MME/AMFs are known as inter-MME/AMF neighbours.
- **Intra-/Inter-MNO/PLMN** Lastly, the highest order of handover in a cellular network is that between MNOs or PLMNs. While a UE is connected to their subscribed MNO/PLMN, any handovers that occur are known as intra-MNO/PLMN handovers. However, when a UE travels to another region not served by their subscribed MNO/PLMN, this is known as inter-MNO/PLMN handover, also known as roaming. Typically this type of handover will occur in regions, jurisdictions or countries that share physical borders.

B. HANDOVER PROCEDURE

The exact processes, exchange of messaging or signalling that occur to execute a handover in the cellular network varies between each of the RRC UE modes (IDLE vs. CONNECTED) [42], [43] and cellular generations (2G, 3G, 4G, 5G) and handover types. However, the overall principle of the handover procedure is the same and is briefly outlined for illustrative purposes:

1) The S-BS and neighbouring BSs continuously transmit reference signals on the downlink channels.
2) The UE performs measurements on the reference signals it can perceive as it travels.
3) The UE periodically generates a measurement report from the conducted measurements.
4) In the RRC IDLE state, the UE will then begin to camp on the most appropriate candidate cell based on the measurement report. Thus, in the RCC IDLE state the procedure is complete. However, in the RRC CONNECTED state, the UE will send the most recently generated measurement report to the S-BS.
5) In the CONNECTED state, the S-BS will make a decision based on the measurement report on whether to begin a handover or not. If so, the S-BS will begin communicating with the most appropriate T-BS to begin the appropriate handover procedure.

C. HANDOVER METRICS

The handover procedure involves communication between a number of different entities in the cellular network i.e., UE, S-BS, T-BS and MME/AMF, as such, there are several different metrics typically used to evaluate the performance of the various processes underlying the handover procedure. A non-exhaustive list of general handover metrics is briefly presented below.

- **Handover Rate:** Measured in Hz, handover rate is the number of handovers per second. Typically, the handover rate can be expected to increase with smaller cell sizes and with higher UE velocities e.g., a car driving through a city.
- **Handover Failure Rate:** Given by Equation 1 [44], handover failures can occur at many points in the handover procedure. Typically, handover failures occur due to poor channel conditions as most handovers will occur at the boundaries between cells.

$$HOFRate = \frac{\#HOFs}{\#HOAttempts} \tag{1}$$

- **Handover Success Rate:** A handover is considered successful if the UE has begun receiving packets from the T-BS without any handover failures occurring since the handover was initiated. The handover success rate is given by Equation 2 [44].

$$HOSRate = \frac{\#HOSs}{\#HOAttempts} \tag{2}$$

- **Ping-pong Rate:** A ping-pong event is the phenomenon wherein a UE will repeatedly perform handovers

between the same S-BS and T-BS. The ping-pong rate is the number of ping-pong events per second.

- **Handover Interruption Time:** The period where a UE cannot send or receive information with the cellular network is known as the Handover Interruption Time (HIT). Typically, handover algorithms attempt to minimise this metric.

In general, a handover algorithm should aim to minimise handover failures, handover rates, ping-pong rates and HIT. As such, minimising these metrics in turn maximises handover successes and therefore results in an average gain in QoS for various network KPIs.

IV. EXPERIMENTAL METHODOLOGY

As previously mentioned, this work aims to expand on the results and findings presented in [16]. Therefore, the experimental methodology that was used to create the dataset for the analysis conducted in this work is described in detail in [16]. However, a brief overview will be presented here to provide context for this work.

A. MEASUREMENT SETUP

Measurements of the cellular network were conducted through a custom application. This application interfaced with two *VirtualAccess* rugged automotive cellular routers; a 4G LTE-only *GW3300* [45] and a 5G NR-enabled *GW1400* [46]. Two types of measurements were collected by the custom application: passive and active. Passive measurements consisted of low-level radio metrics such as serving cell ID, signal strength (Reference Signal Received Strength - RSRP), and signal quality (Reference Signal Received Quality - RSRQ), queried from the router's cellular modem [47], [48] via AT commands. Active measurements were collected by sending ICMP and TCP packets to a remote server, estimating latency and throughput respectively. All measurements conducted were temporally and geo-spatially stamped at the time of collection.

B. MEASUREMENT ROUTES

To reasonably evaluate the commercial cellular network, driving routes were chosen to provide ample coverage of various possible road scenarios. Specifically, four routes were chosen to cover sub-urban, urban, rural and highway scenarios. An overview of these chosen driving routes is provided in Figure 1.

The sub-urban route (centred at 53.285955, −9.066378) follows a ∼4km loop through the University of Galway campus. The urban route (centred at 53.274393, −9.060635) is a ∼13km loop that navigates through the primary roads and junctions in Galway City. The rural route (centred at 53.351526, −9.196307) is a ∼50km loop along the N59 secondary national road to the town of Oughterard (53.429693, −9.318869). The highway route (centred at 53.299666, −8.903497) follows a ∼47km loop along the M6 motorway towards the town of Athenry (53.301198, −8.745321).

V. DATA PROCESSING AND ANALYSIS

As with the analysis performed in the previous work, each of the GPS, active and passive measurements, stored as separate time-stamped trace files are pre-processed before analysis. Initially, simple unit conversions are applied before the separated data traces i.e., GPS, active, and passive, that share the same collection time are synthesised into a composite trace. This pre-processing revealed that the onboard GPS of the cellular routers will only return null values if the vehicle's location remains constant for longer than 1s. As such, these null GPS traces can simply be filled in with the previous known location.

As is discussed in Section III, there are several different metrics used to analyse handover and its effect on network KPIs such as HOF rate, HOS rate, HO frequency and ping-pong rate all rely on access to RRC signalling. RRC signalling could not be collected due to the constraints imposed by the Quectel modems regarding the available commands, response times (300ms) and the network under study being commercial. Additionally, due to the proprietary nature of the network under study, information regarding the implemented architecture and available features of the 4G LTE and 5G NR network could not be ascertained. Consequentially, handover metrics such as HO failure/success rate and interruption time cannot be estimated. However, passive measurements such as current cell ID, ARFCN and current RAT were collected. Therefore, the effect of the aforementioned handover types of intra-/inter-frequency and inter-RAT on end-user latency performance can be analysed. This effect on the end user latency performance is analysed by calculating the relative increase in latency at the time of a handover event. This relative increase in latency is then captured by the difference between the measurement at the time of handover and the cumulative average since the previous handover event as given by Equation 3 [49]:

$$Latency\ Cost = HO_n - \frac{M_{n-1} + \ldots + M_{n-k}}{k} \tag{3}$$

where HO_n is the latency, in milliseconds, measured at the handover event, M_{n-1} is the latency, also in milliseconds, measured before the handover event and k is the number of samples since the previous handover event. It should be noted that only the samples collected since the most recent handover event are considered for each cumulative average calculation to ensure that the samples are locally relevant i.e. within the same cell.

VI. RESULTS

As previously discussed, the analysis in this work aims to estimate and characterise the effect of handover on latency performance of the early 5G NR deployments in V2X scenarios. To do so, we first present and discuss the overall effect of handover on both measurement devices the

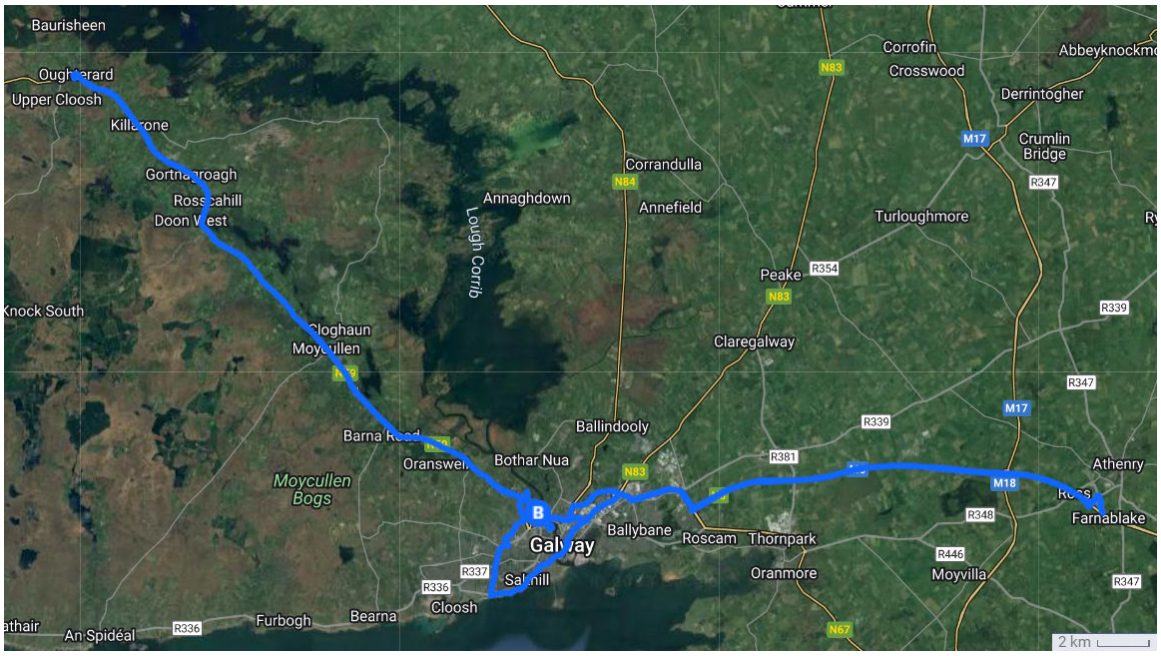

FIGURE 1. Overview map of driving routes throughout galway city region (centred at 53.294080, −9.058970) (Map data ©2023 Google).

5G NR-enabled GW1400 and 4G LTE-only GW3300. Following this, the performance of each of the driving routes outlined in Section IV-B will be compared for each device individually. It should be noted that this work follows the conventions set in the previous work [16], wherein the figures presented in this analysis utilise a log axis for display purposes, however, the analysis is performed irrespective of this. In addition, the upper and lower fences of the box plots presented in this section are determined by Equations 4 & 5, where IQR is the inter-quartile range.

$$LowerFence = Q_1 - 1.5(IQR) \tag{4}$$

$$UpperFence = Q_3 + 1.5(IQR) \tag{5}$$

A. OVERALL COMPARISON

As previously mentioned, latency stands as a vital metric for V2X applications. Delayed data can misguide intelligent vehicles, risking accidents in safety-critical situations and reducing traffic efficiency, fuel economy, and passenger comfort in other cases. Tables 2 and 3, alongside Figures 2 and 3 present the overall latency cost or handover performance statistics and distributions for each of the two cellular routers, 5G NR-enabled GW1400 and 4G LTE-only GW3300, respectively. Additionally, frequency bands observed during the measurement campaign are presented in Table 1.

It should be noted that distributions from latency measurement data tend to have a positive skewness and high kurtosis (leptokurtic) i.e., the mass of the distribution is concentrated to the left of the graph with a long tail to the right, a.k.a heavy-tailed. This is a natural consequence of the fact that latency measurements are by definition constrained to the positive integers and, as a result of significantly delayed packets, can exhibit a larger proportion of outliers with high z-scores.

TABLE 1. Operating frequencies observed during measurement campaign.

RAT	Frequency	Band
3G HSPA	900 MHz	8
	2100 MHz	1
4G LTE	700 MHz	28
	800 MHz	20
	1800 MHz	3
	2100 MHz	1
	2600 MHz	7
5G NR	1800 MHz	n3
	3600 MHz	n78

1) 5G NR-ENABLED GW1400 DEVICE

First, only samples from the 5G NR-enabled GW1400 device are considered, which are detailed in Table 2. As should be expected, there are far fewer (76.9% less) inter-frequency handovers observed compared to intra-frequency handovers. Typically, MNOs have access to a limited number of channels within the cellular bands. As such, it is typical to observe adjacent cells that are intra-frequency neighbours rather than inter-frequency neighbours. However, unexpectedly, there is a notably larger number of inter-RAT handovers observed for the 5G NR-enabled GW1400 device, compared to the other handover types. Inter-RAT handovers would be expected to be minimised in their occurrences due to the cost associated with the degree of control signalling and radio re-tuning required to switch between RATs. The likely rationale for this observation is that the 5G NR-enabled GW1400 device

TABLE 2. Overall statistics for latency cost (ms) due to handover for 5G NR-enabled GW1400 device.

Handover Type	Count	Mean	StD.	Skew	Kurt.	Min.	25%	50%	75%	Max.
Inter-RAT	380	80.78	212.03	8.49	95.80	0.78	20.07	29.60	51.99	2,940.80
Intra-Freq.	325	60.90	118.79	5.58	36.34	0.09	21.07	29.76	43.01	1,076.94
Inter-Freq.	75	72.51	190.70	5.19	30.00	0.37	12.15	25.80	38.78	1,362.47

TABLE 3. Overall statistics for latency cost (ms) due to handover for 4G LTE-only GW3300 device.

Handover Type	Count	Mean	StD.	Skew	Kurt.	Min.	25%	50%	75%	Max.
Intra-Freq.	386	22.14	40.16	6.07	44.39	0.05	7.53	14.13	20.88	423.68
Inter-Freq.	43	41.82	94.75	3.99	17.70	0.24	5.49	13.40	23.59	531.72

will attempt to maintain a connection to the new 5G NR deployments when they are available. However, there are far fewer 5G NR cell deployments compared to the existing 4G LTE network. As a result, two adjacent cells may not be intra-RAT neighbours, forcing the 5G NR-enabled GW1400 device to switch to the existing 4G LTE cell deployments to maintain a connection to the network.

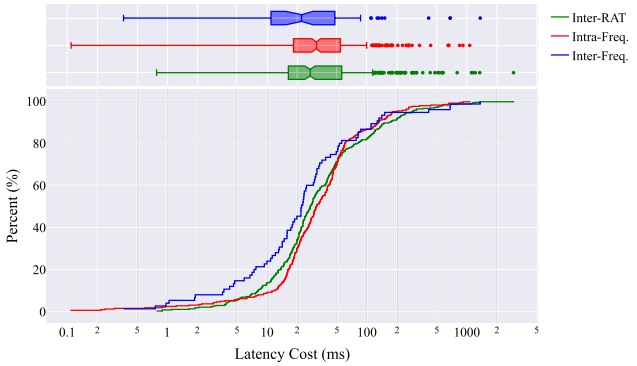

FIGURE 2. eCDF + marginal box plot of latency cost due to handover distribution for 5G NR-enabled GW1400 (Inter-RAT: 29.6ms, Intra-Freq.: 29.76ms, Inter-Freq.: 25.8ms median latency cost).

As can be seen in Table 2, the inter-RAT handover type from the 5G NR-enabled GW1400 device does indeed display on average the highest latency costs of the three detected handover types. This is demonstrated by the larger skewness (8.49) and kurtosis (95.8) of the inter-RAT handovers and is further highlighted by the 2.73x (intra-freq.) and 2.17x (inter-freq.) larger maximum latency cost. From Figure 2, it can be seen that the larger skewness and kurtosis values of the inter-RAT handover type indicate that the distribution has a significantly heavier tail i.e., a larger proportion of outliers, compared to the other two handover types.

Interestingly, the inter-frequency handovers exhibit on average the lowest latency cost of the three detected handover types, as highlighted by the smaller quartiles in Table 2. It should be noted that even though the inter-frequency handover type has a larger mean, standard deviation and maximum sample value compared to the intra-frequency type, this does not indicate poorer performance. As can be seen in the box plot of Figure 2, the intra-frequency handover type is found to have an appreciably larger proportion of outliers than the inter-frequency handover type. This offset seen for the inter-frequency handover type is due to the three outliers, one of which happens to exceed the maximum observed sample value of the intra-frequency handover type.

The inter-RAT handover type has the highest latency cost or worst handover performance of the three handover types, likely due to the higher degree of control signalling and radio adjustments required to execute an inter-RAT handover. This inherent limitation of these inter-RAT handovers could be considered tolerable if they occurred infrequently, however, results reveal that this is not the case and in fact, they are the most commonly observed handover type. It would also be expected that the intra-frequency handover type should have the lowest latency cost given there is less signalling overhead and no radio re-tuning required to perform it. However, this is not what the results indicate. The inter-frequency handover type displays the lowest average latency costs or the best handover performance. This unexpected outcome might stem from a smaller observed sample size for inter-frequency handovers, however, slightly poorer intra-frequency handover performance could be linked to interference. Handovers typically occur at the boundaries between cell regions also known as handover regions. If these handover regions exist in an area with a large degree of occlusions such as buildings and or foliage, the non-line-of-sight (NLOS) and multi-path fading accrued between the serving and target base stations can affect the handover procedure.

2) 4G LTE-ONLY GW3300 DEVICE

Next, only samples from the 4G LTE-only GW3300 device are considered, which are detailed in Table 3. As with the previous work, the 4G LTE-only GW3300 device did not experience any inter-RAT handovers throughout the entire measurement campaign. Similar to the 5G NR-enabled GW1400 device is the trend in the relative frequency of occurrences of the intra-frequency and inter-frequency handover types for the 4G LTE-only GW3300 device. Again as expected, there are far fewer inter-frequency handovers compared to intra-frequency handovers, however, the difference is larger for this device (∼88.8% less). Likely, this increase in the difference in the relative frequency of the two handover types is a product of the maturity of the existing 4G LTE network in the area under study.

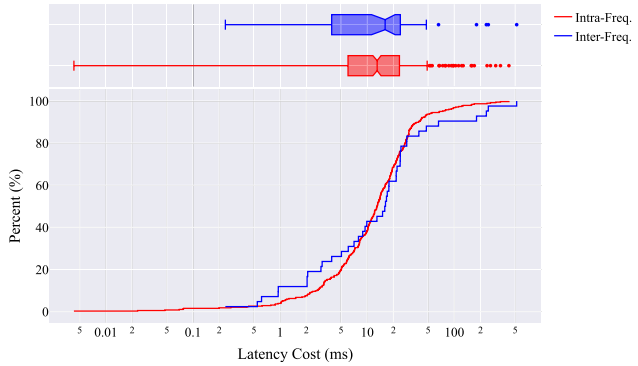

FIGURE 3. eCDF + marginal box plot of latency cost due to handover distribution for 4G LTE-only GW3300 (Intra-Freq.: 14.13ms, Inter-Freq.: 13.4ms median latency cost).

For the 4G LTE-only GW3300, the latency cost or handover performance difference between the handover types is less pronounced than with the 5G NR-enabled GW1400 device. As previously mentioned, the smaller observed sample size of inter-frequency handovers may influence the apparent nuanced behaviour of the distribution. From the empirical CDF plot in Figure 3, it is clear that the inter-frequency handover type achieved a greater percentage of lower latency handovers. This is highlighted by the 25th (intra-freq.: 7.53ms, inter-freq.: 5.59ms) and 50th (intra-freq.: 14.13ms, inter-freq.: 13.4ms) percentiles, shown in Table 3. However, an apparent crossing point between the two handover types occurs in the 40-50% range, indicating a decrease in reliability for the inter-frequency handover type.

This behaviour displayed by the data suggests that if an inter-frequency handover is to occur and is successful, the latency cost will be quite low. However, if the handover is not successful due to a radio link failure or similar issue then the latency cost is significant due to the need to perform a re-connection procedure to the target base stations on the new frequency band. This is further highlighted by the fact that the largest outlier for the inter-frequency handover type (531.72ms) is greater than the largest outlier for the intra-frequency handover type (423.68ms).

3) COMPARISON BETWEEN DEVICES

Finally, samples from both measurement devices are considered to evaluate differences in performance and behaviour. As mentioned previously, no inter-RAT handovers were observed for the 4G LTE-only GW3300 device. As such, no comparison can be drawn between the devices regarding the performance of this handover type. However, the distinct lack of this handover type observed with the 4G LTE-only GW3300 device gives further merit to the need for minimisation of occurrences in new 5G NR deployment strategies, due to the associated control signalling and radio management costs. Moreover, this insight regarding inter-RAT handovers may highlight a strong rationale for the reliability discrepancies found in the previous study conducted on this dataset.

Regarding the other two handover types, it was previously noted that there is a commonality between the two devices regarding the relative frequency of handovers. Particularly of note is the increased difference in this relative frequency of handover types found for the 4G LTE-only GW3300 device. Spectrum access is the likely cause for this increased difference between the measurement devices, as the 5G NR-enabled GW1400 device has access to the same spectrum i.e., frequency bands as the 4G LTE-only GW3300, in addition to the new 5G NR frequency bands.

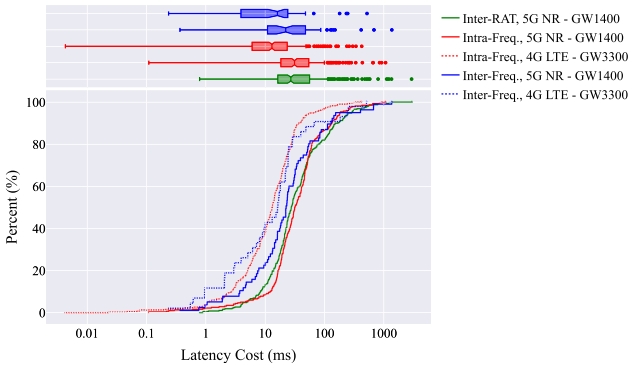

FIGURE 4. eCDF + marginal box plot of latency cost due to handover distribution for both measurement devices.

Tables 2 and 3 illustrate that the 4G LTE-only GW3300 device achieved on average lower latency costs across both the intra-frequency and inter-frequency handover types. This is particularly evident from Figure 4 and the percentiles reported by each device for the intra-frequency handover type. Specifically, the 75th percentile of the 4G LTE-only GW3300 (20.88ms) closely matches the 25th percentile of the 5G NR-enabled GW1400 (20.07ms) showing a marked improvement in latency cost performance.

In addition to improved latency cost performance, the 4G LTE-only GW3300 also exhibits a higher degree of reliability compared to the 5G NR-enabled GW1400, as is highlighted by the lower positive skewness and smaller inter-quartile range across all handover types. This difference in reliability is further highlighted by the fact that the 5G NR-enabled GW1400 device has a significantly larger proportion of outliers and larger maximum values i.e., worst case scenarios (intra-freq.: ∼2.6x, inter-freq.: ∼2.5x increase in maximum latency cost). These findings are confirmed by the results of a Mann-Whitney U Test [49], revealing that there is a significant difference between the latency costs of both devices ($p < 0.001$). Overall, the difference in latency cost performance and reliability between the two measurement devices highlights the degree of ramifications that technology maturity has on QoS.

B. ROUTE COMPARISON

Following the presentation and comparison of the overall latency cost performance of both devices, this subsection will compare the latency cost performance of both devices across each of the four driving routes used to conduct the

measurements. This part of the analysis aims to acquire insights into the processes and mechanisms that influence the performance and behaviours discussed in the previous section. Particularly, key areas of concern will be highlighted for each of the routes as found by each measurement device. It should be noted that an online public coverage map and cell site viewer is provided by the National Commission for Communications Regulation (ComReg) [50].

1) 5G NR - GW1400 DEVICE

First, we consider the samples collected from the 5G NR-enabled GW1400 device. Table 4 presents the descriptive statistics for each of the handover types along each of the driving routes for the 5G NR-enabled GW1400 device.

a: SUB-URBAN ROUTE

Along the Sub-Urban route, we see a continuation of the trend in the relative frequency of the handover types. For this route, there were significantly fewer instances of inter-frequency handovers (∼93%) observed compared to the other two handover types. Almost equal amounts of inter-RAT handovers (83) and intra-frequency handovers (80) were found. The increased difference in relative frequency for this route compared to the overall difference in relative frequency (∼76.9% less) can likely be attributed to the fact that this route does not traverse a significant geographic area. Therefore, the same cells are visited repeatedly, very few of which appear to be inter-frequency neighbours. Due to the lack of samples for the inter-frequency handover type, only the performance of the remaining two handover types can be discussed.

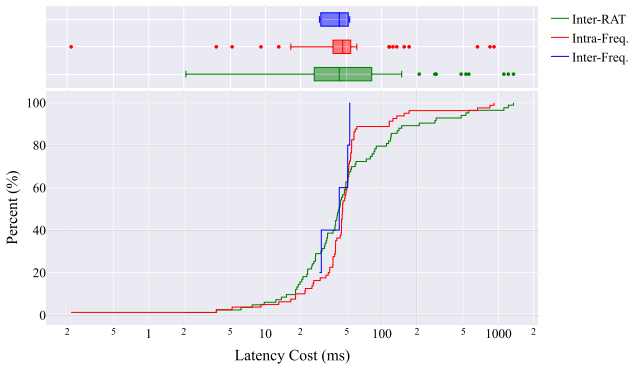

FIGURE 5. eCDF + marginal box plot of latency cost due to handover distribution along the sub-urban route for 5G NR-enabled GW1400 (Inter-RAT: 43.09ms, Intra-Freq.: 46.12ms, Inter-Freq.: 43.12ms median latency cost).

Considering the performance of the remaining two handover types along this route, the data suggests that the inter-RAT handover type has the least performance and reliability. This can be seen from the inter-quartile range (54.59ms) and maximum sample value (1,346.54ms) of this handover type in Table 4, but also more apparent from the box plot in Figure 5. Conversely, the intra-frequency has a much higher degree of reliability as is also shown by its ∼70% smaller inter-quartile range (15.93ms) and lower maximum sample value (916.34ms). However, interestingly, the inter-RAT handover types for this route exhibit similar behaviour to the inter-frequency handovers found for the overall performance of the 4G LTE-only GW3300 device. From the percentiles in Table 4 and the empirical CDF in Figure 5 there is a crossing point between curves the inter-RAT and intra-frequency handover types. This indicates that if an inter-RAT handover is to occur and if it is successful the latency cost will likely be lower than the intra-frequency handover type. However, if some form of handover failure occurs e.g., radio link failures, then the latency cost with be significantly more compared to the intra-frequency handover type.

To gain further insight into the possible causes or underlying processes behind the distributions observed for each of the handover types, features and characteristics of the Sub-Urban Route are explored. Figure 6 presents the scatter plot maps for the handovers observed along this route, where Figure 6(a) provides an overview of the route. Inspection of the overview of the route reveals a large concentration of handovers observed in the highlighted region in the upper middle of the map. Figure 6(b) offers an enlarged view of this specific area. Here, the route traverses Corrib Village (53.288240, −9.066114) and Goldcrest Village (53.288028, −9.066951) student accommodations, characterised by a dense arrangement of buildings and foliage. From Figure 6(b) it can be seen that 4 of the 5 inter-frequency handovers occur in this region along with a significant number of inter-RAT handovers. In fact, ∼68% of the total observed handovers for this route occur within this region. Therefore, it is highly likely that occlusions are the primary source of handovers in this area given the −113dBm mean signal strength (RSRP) value observed at the time of handover within this region. It should be noted that typically RSRP values less than −100dBm are considered to be at the edge of a cell's coverage area, as such, this region of the route can be considered a cell boundary or handover region. Therefore, due to the poor signal strength values measured, the outliers with high latency costs observed for this route are likely a result of radio link failures that occur as the measurement devices attempt to establish a connection to the best cell.

b: URBAN ROUTE

Along the Urban route, there were ∼70-80% fewer instances of inter-frequency handovers observed compared to the other two handover types. There were distinctly more inter-RAT handovers (202) observed compared to intra-frequency handovers (124). This increase in the total number of observed handovers is expected as urban regions like Galway City tend to have a higher density deployment of cells. Also, given that this route traverses a significant portion of the area of Galway City, it is likely that the larger number of inter-RAT handovers relative to the number of intra-frequency handovers is a result of the early 5G NR deployments not yet having complete coverage of the city.

TABLE 4. Route comparison statistics for latency cost (ms) due to handover for 5G NR-enabled GW1400 device.

Route	Handover Type	Count	Mean	StD.	Skew	Kurt.	Min.	25%	50%	75%	Max.
Sub-Urban	Inter-RAT	83	114.79	239.72	3.97	16.18	2.09	26.51	43.09	81.10	1,346.54
	Intra-Freq.	80	77.15	149.47	4.82	23.20	0.22	38.11	46.12	54.04	916.34
	Inter-Freq.	5	41.30	11.23	-0.18	-2.93	29.13	30.24	43.12	50.95	53.04
Urban	Inter-RAT	202	59.11	98.19	4.14	22.05	0.89	16.42	23.83	55.97	799.95
	Intra-Freq.	124	54.05	77.18	4.64	30.37	0.09	17.87	27.46	60.07	653.37
	Inter-Freq.	37	89.64	242.80	4.63	22.68	1.88	13.04	21.87	55.96	1,362.47
Rural	Inter-RAT	42	166.74	478.61	5.16	28.82	7.61	20.16	35.28	96.09	2,940.80
	Intra-Freq.	69	74.74	158.70	4.68	25.01	0.30	16.15	27.68	46.25	1,076.94
	Inter-Freq.	9	144.81	239.86	1.89	2.74	0.37	9.39	33.06	86.40	682.21
Highway	Inter-RAT	50	39.12	69.26	3.09	9.34	0.78	8.72	14.84	24.90	313.92
	Intra-Freq.	52	46.61	65.70	2.40	5.00	0.24	14.23	21.72	41.02	263.96
	Inter-Freq.	24	25.75	33.86	2.51	6.44	0.76	6.24	15.02	32.11	140.94

(a) Overall View of Sub-Urban Route

(b) Magnified View of Corrib Village & Goldcrest Village Student Accommodations

FIGURE 6. Handover type maps of sub-urban driving route through university of galway campus for the 5G NR-enabled GW1400 device (centred at 53.285955, −9.066378) (Map data ©2023 mapbox).

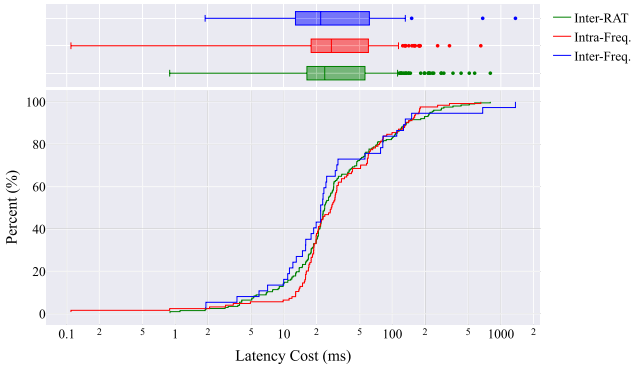

FIGURE 7. eCDF + marginal box plot of latency cost due to handover distribution along the urban route for 5G NR-enabled GW1400 (Inter-RAT: 23.83ms, Intra-Freq.: 27.46ms, Inter-Freq.: 21.87ms median latency cost).

Across the various handover types for this route, the data suggest a relatively consistent level of performance. This can be primarily seen from the similarity in skewness, kurtosis and percentile values in Table 4 and the empirical CDF curves and box plots in Figure 7. However, despite their similarity, there are notable differences between these handover types. Particularly, the inter-frequency type displays the least reliability among the handover types, noted from its larger inter-quartile range (42.92ms) in combination with having the largest outlier or maximum sample value (1,362.47ms). Additionally, the skewness and percentiles indicate that the inter-RAT handover type has marginally higher handover performance compared to the intra-frequency handover type. This can be seen more clearly in the box plot in Figure 7.

Figure 8 presents the scatter plot maps of the handovers observed along the Urban route, to provide insight into the underlying processes behind the behaviour identified for this route. Examination of the overview map in Figure 8(a) reveals that, unlike the concentrated region along the Sub-Urban route, the handover types are quite spread out across the Urban route. This spread of the handover types reveals a compelling rationale for their relatively consistent performance found from the statistical analysis. Additionally, towards the centre of this overview map is a highlighted region of concern for the route. Figure 8(b) provides a magnified view of this region, which encompasses the Spanish Arches (53.269727, −9.054157) and the Claddagh (53.266373, −9.056499) areas of Galway City. As is shown in Figure 8(b) this region was found to have a concentration of handovers, a significant portion of which were inter-RAT handovers. This concentration of handovers indicates that the region is at the boundary between cells, as is highlighted by the −98dBm average signal strength measured in the region. From the perspective of a V2X communications system, this region of the Urban route is of particular concern as it is typically one of the busiest regions of the city in terms of

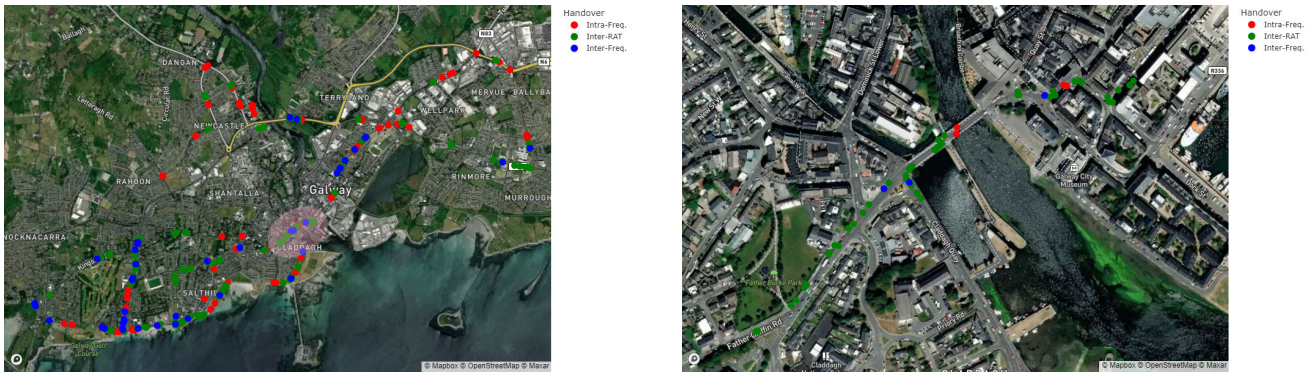

(a) Overall View of Urban Route

(b) Magnified View of the Claddagh and Spanish Arch Area

FIGURE 8. Handover type maps of urban driving route through galway city for the 5G NR-enabled GW1400 Device (centred at 53.274393, −9.060635)(Map data ©2023 mapbox).

pedestrian, cyclist and vehicular traffic. As such, the cells serving this region will likely suffer from congestion which can significantly impact the handover process, particularly in the event of a handover failure, where a re-connection procedure must be performed.

c: RURAL ROUTE

Along the Rural route, ∼80-85% fewer instances of inter-frequency handovers were observed compared to the other two handover types. Unlike the other routes discussed this far, there were substantially more intra-frequency handovers (69) observed compared to inter-RAT handovers (42). This increase in the ratio of intra-frequency handovers to inter-RAT handovers is expected for rural scenarios. It is typical, due to the large coverage areas of cells in these areas, to allow adjacent cells to operate on the same frequency band as the inter-cell interference will be more manageable at the boundaries between cells. Additionally, it is also expected that the total number of handovers for this route is notably lower than the Sub-Urban and Urban routes, given that it is typical that rural cell deployments tend to be more sparse i.e., fewer cell boundaries.

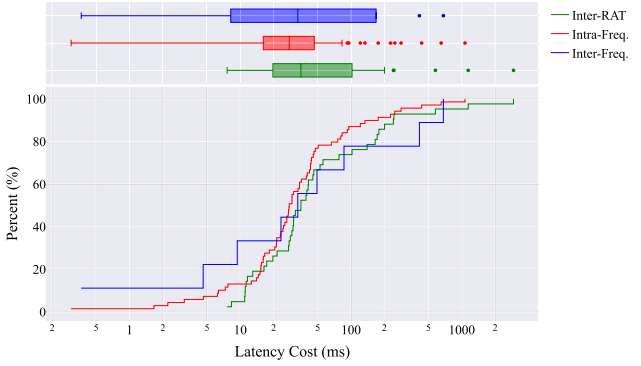

FIGURE 9. eCDF + marginal box plot of latency cost due to handover distribution along the rural route for 5G NR-enabled GW1400 (Inter-RAT: 35.28ms, Intra-Freq.: 27.68ms, Inter-Freq.: 33.06ms median latency cost).

Given the lack of samples for the inter-frequency handover type, only the performance of the inter-RAT and intra-frequency handover types can be compared for this route. The inter-RAT handover type displays worse handover performance and reliability compared to the intra-frequency handover type, as is illustrated in Figure 9. This drop in performance between the two handover types is also evident from the difference in standard deviation (inter-RAT: 478.61ms, intra-freq.: 158.8ms) and the 25th, 50th and 75th percentiles presented in Table 4. While the sample size is not large enough to make definitive claims, the spread of the samples collected for the inter-frequency handovers suggests that this handover type may have similar performance and reliability to the inter-RAT handovers.

The scatter map plots for the Rural route are presented in Figure 10, where Figure 10(a) provides an overview of the handovers observed along the route. It becomes apparent upon review of this overview map, that the majority of the handovers observed along this route occur in the region along the N59 national road where there is an apparent transition from rural to urban at the outskirts of the city. A magnified view of this transition region is presented in Figure 10(b), where ∼62.5% of the total handovers observed for the Rural route was found to occur. Notably, all of the inter-RAT handovers observed for this route occurred within this region. This region along the N59 national road features a gradient of density in terms of housing and foliage as the rural area transitions into the city. This suggests that this region is not only the transition point for environmental factors such as buildings and flora but also for cell deployment patterns, from sparse rural deployments to dense urban deployments. This national road is an example of an artery road used by commuters (pedestrians, cyclists, vehicles) to access the city, thus it is subject to high-speed high-density traffic multiple times a day. As such, this is a key area of concern when considering cellular network planning for V2X communications, particularly when considering the number of vulnerable road users likely to be in this area. Similar to the area of concern along the Urban route, handovers in these transition regions should be minimised given their impact on latency, this is especially pertinent when considering the impact found for the inter-RAT handover type.

(a) Overall View of Rural Route

(b) Magnified View of the N59 and Gortacleva Area

FIGURE 10. Handover type maps of rural driving route to and from oughterard town for the 5G NR-enabled GW1400 Device (centred at 53.351526, −9.196307) (Map data ©2023 mapbox).

d: HIGHWAY ROUTE

A more even ratio of occurrences for each of the handover types is observed along the Highway route, where there are only ∼52% fewer inter-frequency handovers observed. Similar to the Sub-Urban route, the inter-RAT (50) handovers and intra-frequency (52) handovers are similar in frequency. However, unlike the Sub-Urban route, the number of inter-frequency (24) handovers observed is notably larger along the Highway route. This trend observed for the Highway route does not match that which was observed for the Rural route, which initially would be expected to exhibit similar patterns given that both routes follow artery roads out of the city. However, the Highway route follows a motorway road where speed limits are higher than national roads i.e., 100km/h vs. 120km/h. As such, the Highway route features different environmental characteristics i.e., no residential housing along the route and sparse foliage. Therefore, it is likely that the cell deployments along this route are more sparse i.e., larger cell areas, than the Rural route, thus resulting in the relative handover frequency ratios observed.

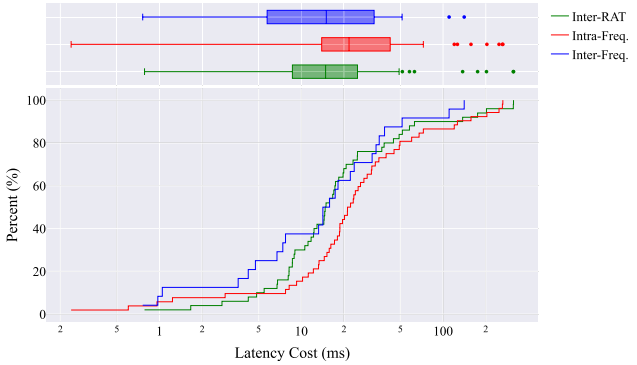

FIGURE 11. eCDF + marginal box plot of latency cost due to handover distribution along the highway route for 5G NR-enabled GW1400 (Inter-RAT: 14.84ms, Intra-Freq.: 21.72ms, Inter-Freq.: 15.02ms median latency cost).

Similar to the Urban route, the handover performance between the handover types along this route is relatively consistent, though the reliability of all handover types is notably higher along this Highway route compared to the Urban route. However, between the handover types, there are notable differences. The inter-frequency handover type displays the best-achieved handover performance and reliability, which is evident from the standard deviation of the 25th (6.24ms), and 50th (15.02ms) percentiles and can be seen in the empirical CDF curves in Figure 11. Conversely, the intra-frequency handover type exhibits the poorest handover performance as shown by the percentiles in Table 4 and the more significant proportion of high latency cost outliers in Figure 11. Additionally, the handover performance and reliability of the inter-RAT handovers are higher than that of intra-frequency handovers, not only as is evident from the box plot in Figure 11, but also by its skewness (inter-RAT: 3.09, intra-freq.: 2.4) and kurtosis (inter-RAT: 9.34, intra-freq.: 5) values. This data suggests, due to the characteristics of this route i.e., high mobility and large cell areas, that it is more challenging to perform intra-frequency handovers. Specifically, for this device, along this Highway route, a mean SINR of 5.27dB (StD: 9.81dB, median: 8dB) was measured during the intra-frequency handovers, which is indicative of the handovers occurring at the boundary between cells [51], [52].

The scatter map plots for the Highway route are presented in Figure 12, where Figure 12(a) provides an overview of the handovers observed along the route. Inspection of this overview map reveals that a large number of intra-frequency handovers are observed near the intersection or crossing point between the M6, M17 and M18 motorway roads. A magnified view of this region is presented in Figure 12(b), where ∼50% of the total handovers observed for the Highway route was found. While there are no notable environmental features such as buildings, foliage or topology changes along this section of the route, the average signal strength found in this region is −105dBm, suggesting that this is a boundary region between cells. As previously mentioned, this Highway route along the M6 motorway is an artery road used by commuters to access the city. Additionally, the M17 and M18 motorway roads are also utilised by commuters from nearby towns to access the M6 into the city. Thus, this intersection

(a) Overall View of Highway Route

(b) Magnified View of the Crossing between the M6, M17 and M18 Motorway Roads

FIGURE 12. Handover type maps of highway driving route to and from athenry town for the 5G NR-enabled GW1400 Device (centred at 53.299666, −8.903497) (Map data ©2023 mapbox).

or crossing point is subject to a large volume of high-speed vehicular traffic multiple times per day, similar to the Rural route. In the context of planning the cellular network for V2X communications, efforts should be directed towards minimising handovers in these areas and similar regions characterised by the convergence of high-speed vehicular traffic.

2) 4G LTE - GW3300 DEVICE

Following the presentation of the route comparison for the 5G NR-enabled GW1400 device, we now consider the samples collected from the 4G LTE-only GW300 device. Table 5 presents the descriptive statistics for each of the handover types along each of the driving routes for the 4G LTE-only GW3300 device.

a: SUB-URBAN ROUTE

Along the Sub-Urban route, there is a sizeable difference in the relative frequency of the two observed handover types, intra-frequency (123) and inter-frequency (2). Due to the lack of samples for the inter-frequency handover type along this route, little can be observed about its effect. Though with the 2 samples that are observed, the latency cost is quite low. This ∼98% difference in handover frequency is likely observed because the existing 4G LTE network has been optimised after many years of deployment. Thus, if any handovers occur, they are only the lowest expected latency cost handover type: intra-frequency handovers.

The data on the intra-frequency handovers suggests quite a high degree of reliability, particularly evident from its large skewness (6.97) and kurtosis (59.66) values alongside a small inter-quartile range (10.32ms) in Table 5. While this large kurtosis does suggest that the mass of the distribution is more concentrated close to the median, it also highlights that the distribution is notably heavy-tailed, as is further shown by the proportion of outliers in the box plot of Figure 13 and by its maximum sample value (423.68) having a z-score of 9.188.

Scatter map plots for this route are presented in Figure 14, where Figure 14(a) provides an overview map of the route.

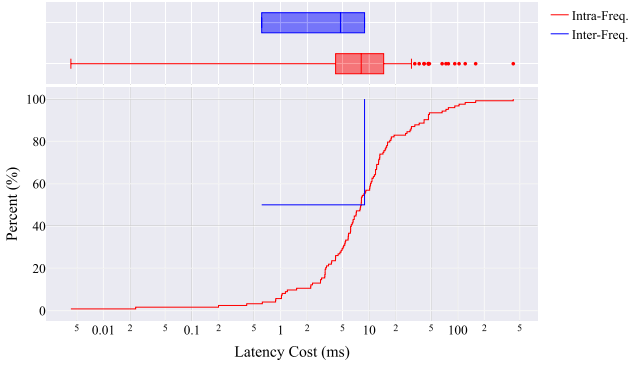

FIGURE 13. eCDF + marginal box plot of latency cost due to handover distribution along the sub-urban route for 4G LTE-only GW3300 (Intra-Freq.: 8.14ms, Inter-Freq.: 4.75ms median latency cost).

Initially, it is clear that there is a very similar pattern of handovers to what was found for the 5G NR-enabled GW1400 device along this route. Particularly, it can be seen there is another distinct grouping of handovers in the segment of this route that passes through the Corrib Village (53.288240, -9.066114) and Goldcrest Village (53.288028, -9.066951) student accommodations. More notable, however, is the area highlighted at the northernmost section of the route in Figure 14(a). This section of the route, magnified in Figure 14(b), encapsulates the Dangan Park & Ride Parking Lot (53.290423, −9.072105).

This parking lot, which serves many of the students and staff of the university, features a large open area entirely encapsulated by tall and dense trees. From the magnified view, a distinct grouping of handovers is observed at the entrance of the parking lot where the dense foliage begins. The average signal strength observed at this entrance to the parking lot is −92dBm which is ∼8.4dBm lower than the average for the entire route. As such, this behaviour aligns with that found for the 5G NR-enabled device for this route. However, this segment of the route is of particular concern for V2X communications as intelligent parking lots are a particularly attractive early system for the technology, due to

TABLE 5. Route comparison statistics for latency cost (ms) due to handover for 4G LTE-only GW3300 device.

Route	Handover Type	Count	Mean	StD.	Skew	Kurt.	Min.	25%	50%	75%	Max.
Sub-Urban	Intra-Freq.	123	19.12	44.03	6.97	59.66	0.003	4.18	8.14	14.50	423.68
	Inter-Freq.	2	-	-	-	-	0.61	-	-	-	8.88
Urban	Intra-Freq.	80	29.06	46.29	4.38	20.22	0.27	14.43	19.48	24.71	298.69
	Inter-Freq.	8	38.22	58.06	2.67	7.37	0.55	14.85	21.10	28.45	179.94
Rural	Intra-Freq.	109	21.41	43.10	5.55	35.38	0.05	4.77	10.36	20.61	338.90
	Inter-Freq.	26	22.67	47.97	4.36	20.45	0.24	2.97	8.91	20.95	245.74
Highway	Intra-Freq.	73	21.91	18.44	3.20	14.83	0.78	11.18	18.16	29.10	126.48
	Inter-Freq.	6	141.47	203.79	1.72	2.45	12.94	21.53	30.36	184.87	531.72

(a) Overall View of Sub-Urban Route (b) Magnified View of the Dangan Park & Ride Parking Lot

FIGURE 14. Handover type maps of sub-urban driving route through university of galway campus for the 4G LTE-only GW3300 device (centred at 53.285955, −9.066378) (Map data ©2023 mapbox).

the low speeds involved. Dense foliage like that observed here has significant scattering effects via multi-path propagations resulting in very noisy and challenging channel conditions.

b: URBAN ROUTE

A continuation in the large difference in the relative frequency of the intra-frequency (80) and inter-frequency (8) is found along the Urban route. Unexpectedly, there are ∼35% fewer intra-frequency handovers found along this route compared to the Sub-Urban route. Again, due to the lack of samples for the inter-frequency handover type along this route, substantiated claims cannot be made about its effect. With the few samples that are observed, it is notable that the latency cost is quite low.

Specifically, it can be noted from the 25th, 50th and 75th percentiles in Table 5 and the empirical CDF curves in Figure 15 that both handovers types appear to have similar performance along the Urban route. Moreover, this data for the Urban route suggests a high degree of reliability for the intra-frequency handover type. This is particularly highlighted by its lower maximum sample value (298.69ms) compared to the worst case observed overall, its small inter-quartile range (10.28ms) and the small proportion of outliers as seen in the box plot of Figure 15.

To provide insight into the underlying processes behind the behaviour identified for this route, Figure 14 presents the scatter plot maps of the handovers observed along the Urban route. Examination of the overview map in Figure 14(a) shows that the inter-frequency handovers measured for

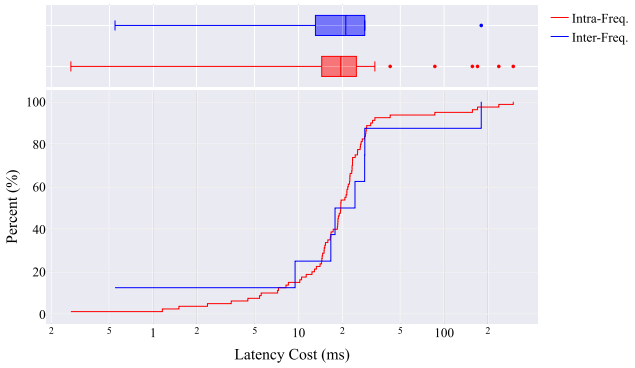

FIGURE 15. eCDF + marginal box plot of latency cost due to handover distribution along the urban route for 4G LTE-only GW3300 (Intra-Freq.: 19.48ms, Inter-Freq.: 21.1ms median latency cost).

this route are quite spread out, indicating the boundaries between macro-cells. Additionally, there is a concentration of handovers observed in the highlighted region in Figure 16(a). Figure 16(b) provides a magnified view of this region, which follows along the Bohermore road (53.278900, −9.044682) that serves as a main access road to the city centre. This route primarily features a high density of primarily residential buildings and is typically subject to high-density pedestrian and vehicular traffic. This concentration of handovers, which encompasses ∼23% of all handovers observed along this route, indicates that the region is at the boundary between cells, particularly where the medium-density cell deployments of the outer city transition into the high-density

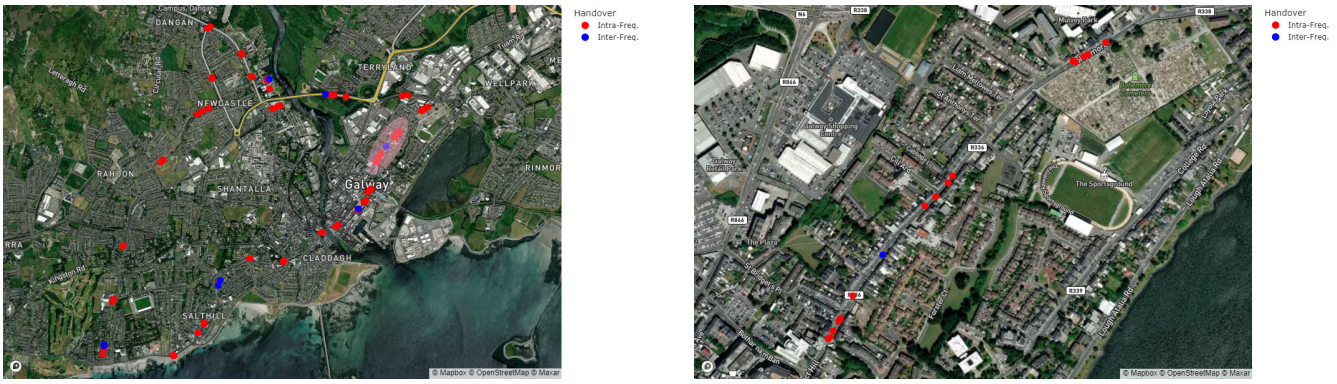

(a) Overall View of Urban Route

(b) Magnified View of the Bohermore Road

FIGURE 16. Handover type maps of urban driving route through galway city for the 4G LTE-only GW3300 device (centred at 53.274393, −9.060635)(Map data ©2023 mapbox).

cell deployments of the city centre. As such, similar to the region identified for the Rural route observed by the 5G NR-enabled GW1400 device, any segment of road that exhibits a high density of handovers, particularly those that are transition regions in cell density should be considered an area of concern. This is especially pertinent when the environment where the handover region occurs features significant static and dynamic obstructions, as highlighted by an 11.65% average increase in latency cost that was observed in regions of low quality (SINR < 13dB [52]).

c: RURAL ROUTE

Along the Rural route, the largest number of inter-frequency (26) handovers is observed along with a substantial number of intra-frequency (109) handovers resulting in a ∼76% difference. While there are still few samples observed for the inter-frequency, there are enough samples observed for this route to more substantially support the descriptive statistics found.

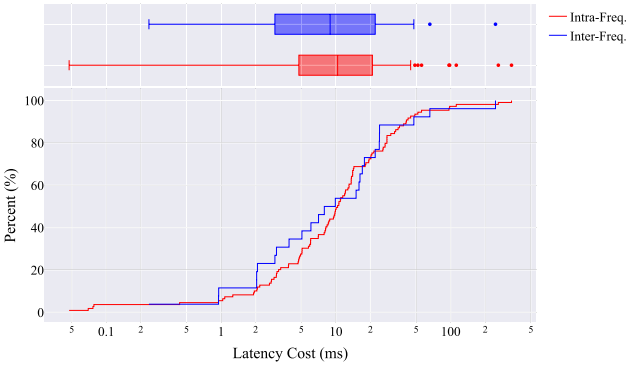

FIGURE 17. eCDF + marginal box plot of latency cost due to handover distribution along the rural route for 4G LTE-only GW3300 (Intra-Freq.: 10.36ms, Inter-Freq.: 8.91ms median latency cost).

As with the Urban route, despite the lack of samples for the inter-frequency handovers, the empirical CDF curves in Figure 17 alongside the percentiles in Table 5 suggest that both handover types have similar handover performance and reliability. There is a notable difference in the size of the inter-quartile range for the inter-frequency handover (17.98ms) type, suggesting that they are less reliable than the intra-frequency handover (15.84ms) type, however, this difference can likely be attributed to the sample sizes. As expected, however, the overall performance of handovers along this route is higher than that found for the Urban route due to the larger handover regions typically experienced in more sparse cell deployments.

The scatter map plots for the Rural route are presented in Figure 18, where Figure 18(a) provides an overview of the handovers observed along the route. It is immediately apparent upon inspection of the overview map, that the majority of the handovers observed along this route occur at the beginning, exactly as was found for the 5G NR-enabled GW1400 device. Similar to the other measurement device, ∼55% of the total handovers observed for the Rural route were to occur in this region. Aside from this region, there is another notable concentration of handovers in the highlighted region of Figure 18(a) just north of the town of Moycullen (53.339190, −9.179954) along the N59 national road. A magnified view of this region, known as Lahardane (53.358663, −9.215534), is presented in Figure 18(b) where two distinct groupings of intra-frequency handovers are observed. It is along this segment of road that the topology of the landscape begins to transition from flat to more hilly terrain. While the previous region clearly has a more significant impact on the handover performance observed along this route, this alternate region highlights another archetype area of concern i.e., adverse geographic topologies, when considering cellular network planning for V2X communications. As such, careful consideration needs to be given when deploying cells to supply adequate coverage to these segments of the road.

d: HIGHWAY ROUTE

Lastly, along the Highway route, the fewest total number of handovers among all the routes for the 4G LTE-only GW3300 device is observed. As with previously discussed, there are too few samples of the inter-frequency handover

(a) Overall View of Rural Route

(b) Magnified View of the N59 and Lahardane Area

FIGURE 18. Handover type maps of rural driving route to and from oughterard town for the 4G LTE-only GW3300 Device (centred at 53.351526, −9.196307) (Map data ©2023 mapbox).

(6) type to support the descriptive statistics in Table 5. However, from these few samples, the data suggests that this handover type performs more poorly than the intra-frequency handover type. Conversely, the intra-frequency handover type for this route displays the highest reliability across all the measurement routes. This is particularly highlighted by the very small proportion of outliers found for this handover type in Figure 19.

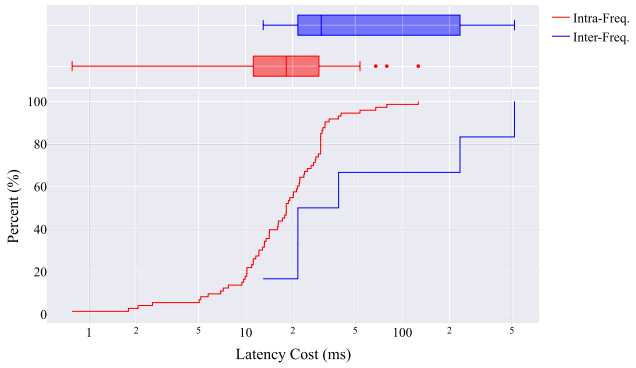

FIGURE 19. eCDF + marginal box plot of latency cost due to handover distribution along the highway route for 4G LTE-only GW3300 (Intra-Freq.: 18.16ms, Inter-Freq.: 30.36ms median latency cost).

The scatter map plots for the Highway route are presented in Figure 20, where Figure 20(a) provides an overview of the handovers observed along the route. Examination of this overview map reveals the same pattern in handovers that was observed by the 5G NR-enabled GW1400 device, where a large number of intra-frequency handovers and all of the inter-frequency handovers for the route are observed near the intersection or crossing point between the M6, M17 and M18 motorway roads. Additionally, at the opposite side of the route, in the highlighted area of Figure 20(b), are another cluster of intra-frequency handovers where the M6 Motorway passes between the Deerpark Industrial Estates (53.280227, −8.928238) and Galway Airport (53.302318, −8.940830). A magnified view of this region is presented in Figure 20(b), where ∼53% of the total handovers observed for the Highway route was found.

Similar to the crossing point discussed previously for the route, there are no notable environmental features such as buildings, foliage or topology changes along this section of the route. However, there are cell sites found at Galway Airport (53.302318, −8.940830) and within the Deerpark Industrial Estates (53.280227, −8.928238). Therefore, the handover clusters observed are a manifestation of an overlap region between two cells, where the handover algorithm is attempting to maintain the best connection to the cellular network. As such, this renders this region another area of concern for V2X communications as either cell deployment would be sufficient to cover this segment of the road, given their proximity to the motorway road. From the perspective of V2X communications, unnecessary handovers should be minimised via make-before-break handover techniques like CHO [29] in addition to cell deployments that optimise coverage for road networks, particularly where there is likely to be high-density high-speed vehicular traffic.

C. DISCUSSION

From the results and findings presented, it is clear that the handover procedure imposes a significant latency cost from an end-user perspective. Particularly, the results here provide a deeper insight into the reliability disparity found between the new 5G NR deployments and the existing 4G LTE network found in the previous work. In fact, it is now apparent that the inter-RAT handover type, which requires the most control signalling and radio management to perform, is the largest source of unreliability for the new 5G NR deployments. This is only further reinforced by the fact that the 4G LTE-only GW3300 device, which measured the existing 4G LTE network, experienced no inter-RAT handovers for the entire duration of the measurement campaign. Additionally, the existing 4G LTE network was found to have on average lower latency costs or improved handover performance across both intra-frequency and inter-frequency handovers. These insights speak to the importance of localised optimisation of cell deployments, which the existing 4G LTE network has had many years of iterative improvement to draw upon.

(a) Overall View of Highway Route

(b) Magnified View of the M6 Motorway near Galway Airport

FIGURE 20. Handover type maps of highway driving route to and from athenry town for the 4G LTE-only GW3300 Device (centred at 53.299666, −8.903497) (Map data ©2023 Mapbox).

These results and findings further reinforce the insights of the previous work regarding the degree of variability between the different measurement routes used to conduct this study. Notably, it was found across both measurement devices that the Highway route displayed not only consistent performance across all three handover types but also on average the lowest latency costs or highest handover performance. Additionally, it was found that the Sub-Urban and Urban routes exhibited on average the least reliability in terms of handover performance. This highlights the degree of impact that both static obstructions, from buildings and foliage, and cell density have on handover performance. Between the different handover types, it would be expected, due to the degree of control signalling and coordination required, that the inter-RAT handover type would perform the poorest and the intra-frequency handover type would perform the best. Contrary to these expectations, the inter-RAT handover doesn't always show the worst performance, and the intra-frequency handover doesn't always exhibit the best performance across all routes and scenarios. It was instead found that factors such as cell deployment density and environmental factors that affect received signal strength and quality were likely to impact the performance of the intra-frequency and inter-frequency handover types.

Furthermore, these varying specific factors that distinguish different V2X scenarios have been highlighted through the discussion on areas of concern. The primary feature of these areas of concern is that they are regions where concentrations of handovers are found, thus indicating that a weakness in the handover algorithms is being exploited. Most notable are regions with significant obstructions i.e., buildings, foliage, and topology, that happen to align will cell boundaries or artificially impose a cell boundary due to occlusions. Given the effect of the areas of concern discussed in this work, such as the student accommodations found along the Sub-Urban route, handover algorithms should be one of the primary focuses of the planning and development of networking for V2X communications.

Given all the findings and insights from this study, it is clear that major systemic improvements are required to address these reliability concerns in order to enable V2X communications as a potential ITS and telecommunications industry vertical. There exist many channels of research aimed at addressing the challenges associated with the handover process, many of which, such as dual connectivity (DC) and conditional handover (CHO) have very promising potential. However, as was made clear by the analysis of the various measurement routes, V2X communications scenarios tend to feature quite a broad collection of variables e.g., static obstructions, geographic topology and dynamic traffic/obstructions, that influence the effectiveness of handover algorithms. As such, it is likely more pertinent to consider incorporating crowd-sourced localised information into not only the prediction and decision processes of the improved generalised handover algorithms utilised across the cellular network but also into the vehicle itself.

From the previous work, it was demonstrated that the average latency performance of the cellular network varies significantly from scenario to scenario and to address these variations would require further development of the 5G NR network. As a result, it was proposed that an Application Map should be developed to inform the connected intelligent vehicle what degree of automation the V2X communications system could support. This application would manifest as segmentation of the road network where regions of high performance and reliability are designated as high-automation regions and vice versa. This work builds upon the Application Map concept as the statistical analysis presented herein can be used to replicate the methods of Toril et al. [24], where statistical models of the handover performance of the road network can be generated. Using techniques like the Maximum Likelihood Estimation (MLE) and Kolmogorov-Smirnov goodness-of-fit tests to fit distributions such as the lognormal and generalised extreme value (GEV) would allow for a high degree of granularity to these Application Maps. These statistical models only require 2-3 parameters and as a result would be easy to disseminate and can be used to

apply confidence intervals to the degree of automation the V2X communications system can support. Therefore, with a probabilistic Application Map a connected intelligent vehicle can increase its safety and traffic efficiency capabilities by either adjusting its level of automation, driving behaviour or intended route.

VII. LIMITATIONS AND FUTURE WORK

As with the work completed previously [16], the results and findings presented in this work are also primarily limited by the practical limitations of using a single test vehicle to conduct measurements. As such, only a portion of the total road network within the coverage of an MNO can be covered. Also, as previously mentioned, given that the network under study was a commercial network, RRC signalling and other handover procedure information cannot be obtained. As a consequence, the cellular network must be treated as a black box system and therefore the results reflect only the end user's experience. Regardless of these limitations, the outlined methods, analysis techniques, results and insights can be used to advise MNOs and automotive manufacturers on the characteristics and behaviours that need to be considered to develop V2X communications as an industry vertical.

In future, the current dataset can be expanded to encapsulate not only more of the available road network but also capture different times of day, days of the week and seasons of the year. This can be achieved by the inclusion of an increased number of test vehicles across several MNOs with varying levels of 5G NR deployments. Consequentially, this would allow for a more granular analysis regarding the effect of handover as it occurs in particular regions of interest such as heavily occluded areas near forests or deep within the city. In addition to static obstructions, a deeper analysis of other contributing factors such as dynamic obstructions, environmental factors and vehicle telemetries can be carried out to isolate the parameters that have the largest impact on the various network KPIs outlined in the standards generated by the 3GPP [8], [53]. Additionally, the current dataset can be used to inform the parameters of a simulation study to provide an analysis of the methods and techniques discussed to mitigate unnecessary handovers and handover failures.

VIII. CONCLUSION

In this work, we present an analysis of the effect of handover on latency in V2X scenarios in early 5G NR deployments. A driving-based measurement campaign was conducted to perform this analysis and was achieved by collecting passive and active network measurements from two cellular routers; one with 5G NR capabilities and the other without, installed in a test vehicle. This test vehicle was driven through several V2X scenario archetypes including Sub-Urban, Urban, Rural and Motorway areas to provide a reasonable representation of typical driving environments.

The results elaborated above demonstrate the substantial latency cost of the handover procedure from an end-user viewpoint. Results also reveal a reliability gap between new 5G NR deployments and the previous 4G LTE network, with the inter-RAT handover type emerging as the main source of unreliability (10-24% higher latency cost) for 5G NR due to demanding control signalling and radio management. Conversely, the 4G LTE-only GW3300 device experienced no inter-RAT handovers, highlighting the superior handover performance, in terms of latency cost, of the existing 4G LTE network for intra-frequency (63% lower) and inter-frequency (36% lower) handovers. This accentuates the need for localised optimisation, which was leveraged during the iterative improvements of the 4G LTE network.

Furthermore, this work reinforces earlier insights into route-based performance variability. Notably, for the 5G NR-enabled GW1400 device, the Highway route consistently demonstrated the lowest average latency costs across all handover types (inter-RAT: 57.5%, intra-freq: 30.1%, inter-freq.: 63.6% lower), while the Sub-Urban and Urban routes exhibited less reliability due to factors such as obstructions and cell density. Interestingly, the expectation that inter-RAT handovers would perform worst and intra-frequency handovers would perform best in all scenarios is overturned. Instead, factors like cell deployment density and environmental conditions were found to significantly influence intra-frequency and inter-frequency handover performance.

Consequentially, these findings emphasise the need for substantial systemic improvements to address reliability concerns, particularly for safety-critical V2X communications. Adoption of make-before-break CHO algorithms, alongside the deployment of cells to optimise coverage for road networks, would constitute the most pertinent improvements for upholding QoS requirements. The complex array of variables impacting handover algorithms in diverse V2X scenarios also suggests the value of integrating crowd-sourced localised information into both the CHO algorithms within the cellular network and vehicles themselves. Additionally, the concept of the Application Map may aid in informing intelligent vehicles of achievable automation levels, building on statistical analysis to create models of handover performance across the road network.

REFERENCES

[1] Cruise. (Aug. 2023). *Cruise Self Driving Cars*. [Online]. Available: https://getcruise.com/

[2] Waymo. (Aug. 2023). *Waymo Driver*. [Online]. Available: https://waymo.com/waymo-driver/

[3] Tesla. (Aug. 2023). *Artificial Intelligence & Autopilot*. [Online]. Available: https://www.tesla.com/AI

[4] Uber. (Aug. 2023). *Uber AV*. [Online]. Available: https://www.uber.com/us/en/autonomous/

[5] *Release 16. 3GPP*. Accessed: Aug. 2023. [Online]. Available: https://www.3gpp.org/release-16

[6] *Release 17. 3GPP*. Accessed: Aug. 2023. [Online]. Available: https://www.3gpp.org/release-17

[7] *IEEE Draft Standard for Information technology—Telecommunications and Information Exchange Between Systems Local and Metropolitan Area Networks–Specific Requirements—Part 11: Wireless LAN Medium Access Control (MAC) and Physical Layer (PHY) Specifications Amendment: Enhancements for Next Generation V2X*, Standard 802.11bd, 2022.

[8] *Service Requirements for V2X Services*, Standard 3GPP TS 22.185, Mar. 2017.

[9] (Aug. 2023). *3GPP*. [Online]. Available: https://www.3gpp.org/

[10] J. Santa, A. F. Gómez-Skarmeta, and M. Sánchez-Artigas, "Architecture and evaluation of a unified V2V and V2I communication system based on cellular networks," *Comput. Commun.*, vol. 31, no. 12, pp. 2850–2861, Jul. 2008.
[11] *Release 14. 3GPP*. Accessed: Aug. 2023. [Online]. Available: https://www.3gpp.org/release-14
[12] *Release 15. 3GPP*. Accessed: Aug. 2023. [Online]. Available: https://www.3gpp.org/release-15
[13] M. Akselrod, N. Becker, M. Fidler, and R. Luebben, "4G LTE on the road–what impacts download speeds most?" in *Proc. IEEE 86th Veh. Technol. Conf. (VTC-Fall)*, Sep. 2017, pp. 1–6.
[14] M. Lauridsen, L. C. Gimenez, I. Rodriguez, T. B. Sorensen, and P. Mogensen, "From LTE to 5G for connected mobility," *IEEE Commun. Mag.*, vol. 55, no. 3, pp. 156–162, Mar. 2017.
[15] S. Neumeier, E. A. Walelgne, V. Bajpai, J. Ott, and C. Facchi, "Measuring the feasibility of teleoperated driving in mobile networks," in *Proc. Netw. Traffic Meas. Anal. Conf. (TMA)*, Jun. 2019, pp. 113–120.
[16] J. Clancy, D. Mullins, B. Deegan, J. Horgan, E. Ward, P. Denny, C. Eising, E. Jones, and M. Glavin, "Feasibility study of V2X communications in initial 5G NR deployments," *IEEE Access*, vol. 11, pp. 75269–75284, 2023.
[17] *Service Requirements for the 5G System*, Standard 3GPP TS 22.261, 2021.
[18] M. Tayyab, X. Gelabert, and R. Jäntti, "A survey on handover management: From LTE to NR," *IEEE Access*, vol. 7, pp. 118907–118930, 2019.
[19] E. Gures, I. Shayea, A. Alhammadi, M. Ergen, and H. Mohamad, "A comprehensive survey on mobility management in 5G heterogeneous networks: Architectures, challenges and solutions," *IEEE Access*, vol. 8, pp. 195883–195913, 2020.
[20] S. Alraih, R. Nordin, A. Abu-Samah, I. Shayea, and N. F. Abdullah, "A survey on handover optimization in beyond 5G mobile networks: Challenges and solutions," *IEEE Access*, vol. 11, pp. 59317–59345, 2023.
[21] R. Bertolini and M. Maman, "Evaluating handover performance for end-to-end LTE networks with OpenAirInterface," in *Proc. IEEE 94th Veh. Technol. Conf. (VTC-Fall)*, Sep. 2021, pp. 1–5.
[22] E. Pareth, "V2X-enabled control of connected vehicles over a 5G network," M.S. thesis, Dept. Inf. Technol. Elect. Eng., ETH Zurich, Zürich, Switzerland, Mar. 2022. Accessed: Jan. 2023. [Online]. Available: https://www.research-collection.ethz.ch/handle/20.500.11850/593447
[23] J. Sultan, M. S. Mohsen, N. S. G. Al-Thobhani, and W. A. Jabbar, "Performance of hard handover in 5G heterogeneous networks," in *Proc. 1st Int. Conf. Emerg. Smart Technol. Appl. (eSmarTA)*, Aug. 2021, pp. 1–7.
[24] M. Toril, V. Wille, S. Luna-Ramírez, M. Fernández-Navarro, and F. Ruiz-Vega, "Characterization of radio signal strength fluctuations in road scenarios for cellular vehicular network planning in LTE," *IEEE Access*, vol. 9, pp. 33120–33131, 2021.
[25] B. Sliwa and C. Wietfeld, "Empirical analysis of client-based network quality prediction in vehicular multi-MNO networks," in *Proc. IEEE 90th Veh. Technol. Conf. (VTC-Fall)*, Sep. 2019, pp. 1–7.
[26] E. A. Walelgne, J. Manner, V. Bajpai, and J. Ott, "Analyzing throughput and stability in cellular networks," in *Proc. NOMS - IEEE/IFIP Netw. Oper. Manage. Symp.*, Taipei, Taiwan, Apr. 2018, pp. 1–9.
[27] A. Gaber, W. Nassar, A. M. Mohamed, and M. K. Mansour, "Feasibility study of teleoperated vehicles using multi-operator LTE connection," in *Proc. Int. Conf. Innov. Trends Commun. Comput. Eng. (ITCE)*, Feb. 2020, pp. 191–195.
[28] Z. Fernández, A. Martín, J. Pérez, M. García, G. Velez, F. Murciano, and S. Peters, "Challenges and solutions for service continuity in inter-PLMN handover for vehicular applications," *IEEE Access*, vol. 11, pp. 8904–8919, 2023.
[29] H.-S. Park, Y. Lee, T.-J. Kim, B.-C. Kim, and J.-Y. Lee, "Handover mechanism in NR for ultra-reliable low-latency communications," *IEEE Netw.*, vol. 32, no. 2, pp. 41–47, Mar. 2018.
[30] J. Stanczak, U. Karabulut, and A. Awada, "Conditional handover in 5G–principles, future use cases and FR2 performance," in *Proc. Int. Wireless Commun. Mobile Comput. (IWCMC)*, May 2022, pp. 660–665.
[31] H.-S. Park, Y. Lee, T.-J. Kim, B.-C. Kim, and J.-Y. Lee, "Faster recovery from radio link failure during handover," *IEEE Commun. Lett.*, vol. 24, no. 8, pp. 1835–1839, Aug. 2020.
[32] S. Bin Iqbal, A. Awada, U. Karabulut, I. Viering, P. Schulz, and G. P. Fettweis, "On the modeling and analysis of fast conditional handover for 5G-advanced," in *Proc. IEEE 33rd Annu. Int. Symp. Pers., Indoor Mobile Radio Commun. (PIMRC)*, Sep. 2022, pp. 595–601.
[33] S. B. Iqbal, S. Nadaf, A. Awada, U. Karabulut, P. Schulz, and G. P. Fettweis, "On the analysis and optimization of fast conditional handover with hand blockage for mobility," *IEEE Access*, vol. 11, pp. 30040–30056, 2023.
[34] F. Zhao, H. Tian, G. Nie, and H. Wu, "Received signal strength prediction based multi-connectivity handover scheme for ultra-dense networks," in *Proc. 24th Asia–Pacific Conf. Commun. (APCC)*, Nov. 2018, pp. 233–238.
[35] C. Lee, H. Cho, S. Song, and J.-M. Chung, "Prediction-based conditional handover for 5G mm-wave networks: A deep-learning approach," *IEEE Veh. Technol. Mag.*, vol. 15, no. 1, pp. 54–62, Mar. 2020.
[36] V. Mishra, D. Das, and N. N. Singh, "Novel algorithm to reduce handover failure rate in 5G networks," in *Proc. IEEE 3rd 5G World Forum (5GWF)*, Sep. 2020, pp. 524–529.
[37] K. Qi, T. Liu, C. Yang, S. Suo, and Y. Huang, "Dual connectivity-aided proactive handover and resource reservation for mobile users," *IEEE Access*, vol. 9, pp. 36100–36113, 2021.
[38] Y. Zhao and X. Zhang, "Smart handover scheme for a 5G-enabled ambulance," in *Proc. 14th Int. Conf. Wireless Commun. Signal Process. (WCSP)*, Nov. 2022, pp. 281–286.
[39] M. Das, A. Singh, P. N. Sreenivas, G. Ponnamreddy, and S. Ganesh, "Optimizing NR handover by using Doppler shift along with legacy power level algorithm," in *Proc. IEEE Int. Conf. Electron., Comput. Commun. Technol. (CONECCT)*, Jul. 2022, pp. 1–5.
[40] L. Yang, M. Cheng, J. Qu, and Z. Chen, "GraphHO: A graph-based handover optimization system for cellular networks," in *Proc. Int. Symp. Wireless Commun. Syst. (ISWCS)*, Oct. 2022, pp. 1–6.
[41] K. Mannem, P. N. Rao, and S. C. M. Reddy, "Multi-objective artificial flora algorithm based optimal handover scheme for LTE-advanced networks," in *Proc. 6th Int. Conf. Electron., Commun. Aerosp. Technol.*, Dec. 2022, pp. 1400–1406.
[42] *Evolved Universal Terrestrial Radio Access (E-UTRA); Radio Resource Control (RRC); Protocol Specification*, Standard 3GPP TS 36.331, Oct. 2018.
[43] *NR; Radio Resource Control (RRC); Protocol Specification*, Standard 3GPP TS 38.331, Oct. 2018.
[44] *Evolved Universal Terrestrial Radio Access (E-UTRA); Mobility Enhancements in Heterogeneous Networks*, Standard 3GPP TR 36.839, Jul. 2013.
[45] VirtualAccess. (Aug. 2023). *GW3300 Series Router*. [Online]. Available: https://virtualaccess.com/gw3000-series/
[46] VirtualAccess. (Aug. 2023). *GW1450 Series 5G Router*. [Online]. Available: https://virtualaccess.com/gw1450-series-5g-router/
[47] Quectel. (Aug. 2023). *5G RM50xQ Series Modem*. [Online]. Available: https://www.quectel.com/product/5g-rm50xq-series
[48] Quectel. (Aug. 2023). *Lte EG25-G Modem*. [Online]. Available: https://www.quectel.com/product/lte-eg25-g
[49] W. Navidi, *Statistics for Engineers and Scientists*. New York, NY, USA: McGraw-Hill, 2011. [Online]. Available: https://books.google.ie/books?id=9yA8PwAACAAJ
[50] N. C. for Communications Regulation. (Jul. 2023). *Cruise Self Driving Cars*. [Online]. Available: ComRegSiteViewer
[51] T. Novlan, J. G. Andrews, I. Sohn, R. K. Ganti, and A. Ghosh, "Comparison of fractional frequency reuse approaches in the OFDMA cellular downlink," in *Proc. IEEE Global Telecommun. Conf. (GLOBECOM)*, Dec. 2010, pp. 1–5.
[52] M. H. A. Khan, J.-G. Chung, and M. H. Lee, "Downlink performance of cell edge using cooperative BS for multicell cellular network," *EURASIP J. Wireless Commun. Netw.*, vol. 2016, no. 1, p. 56, Feb. 2016, doi: 10.1186/s13638-016-0537-0.
[53] *Service Requirements for Enhanced V2X Scenarios*, Standard 3GPP TS 22.186, Nov. 2020.

JOSEPH CLANCY received the B.Eng. degree (Hons.) from the University of Galway, in 2019, where he is currently pursuing the Ph.D. degree. His research interests include wireless communications and network architectures for intelligent transport systems (ITS). He is also a member of the Connaught Automotive Research (CAR) Group under the supervision of Prof. Martin Glavin and Prof. Edward Jones.

DARRAGH MULLINS received the B.E. degree in energy systems engineering and the Ph.D. degree in electronic engineering from the University of Galway, in 2013 and 2018, respectively. His Ph.D. research topic involved the application of imaging sensors and signal processing to wastewater treatment plant performance sensing. He was a Postdoctoral Research Fellow with the University of Galway, from 2018 to 2022, where he managed a research program and co-supervised six Ph.D. student projects involving sensors and V2X communication systems for pedestrian and vehicle monitoring from both vehicle and fixed infrastructure point-of-view. He is currently a Senior Technical Officer and an Adjunct Lecturer with the School of Engineering, University of Galway. He was awarded Lero Director's Prize for Education and Public Engagement, in 2020.

ENDA WARD received the B.E. degree in electronic engineering from the University of Galway, in 1999, and the master's (M.Eng.Sc.) degree in research and in electronic engineering, in 2002, with a focus on biomedical electronics. He is currently responsible for defining the camera product roadmap for surround and automated driving applications within Valeo and has worked with key technology experts across the supply chain and within OEMs to define optimal system architectures. Lecturing for a number of years in the areas of electronics and computing systems with Atlantic Technological University, Ireland, he later moved into industry, working in the biomedical space and has spent the last 16 years in automotive ADAS design. He holds several patents in the area of automotive vision.

PATRICK DENNY (Member, IEEE) received the B.Sc. degree in experimental physics and mathematics from NUI Maynooth, Ireland, in 1993, the M.Sc. degree in mathematics from the University of Galway, Ireland, in 1994, and the joint Ph.D. degree in physics from the University of Galway, in 2000, while researching electromagnetic planetary physics from GFZ Potsdam, Germany. From 1999 to 2001, he was a RF Engineer with AVM GmbH, Germany, designing and developing the hardware for the first integrated GSM/ISDN/USB modem. After working in supercomputing development with Compaq/Hewlett Packard, from 2001 to 2002, he joined Connaught Electronics Ltd. (subsequently Valeo), Tuam, Ireland, as the Team Leader of Radio Frequency Design. Over the next 20 years, he was a Senior Expert with Valeo, designing and developing novel radio frequency and imaging systems, including the first mass production high dynamic range automotive camera, for leading car companies. In 2010, he became an Adjunct Professor in automotive electronics with the University of Galway. In 2022, he became an Associate Professor in artificial intelligence with the Department of Electronic and Computer Engineering, University of Limerick, Ireland. His research interests include automotive imaging technology and its extension into other domains, algorithmic design, artificial intelligence, applied mathematics, and the industrialization of advanced technologies.

EDWARD JONES (Senior Member, IEEE) received the B.E. and Ph.D. degrees in electronic engineering from the University of Galway, Ireland. His Ph.D. research topic was on the development of computational auditory models for speech processing. He is currently a Professor in electrical and electronic engineering with the School of Engineering, University of Galway. From 2009 to 2010, he was a Visiting Researcher with the Department of Electrical Engineering, Columbia University, New York City, NY, USA, and has also been appointed as a Visiting Fellow with the School of Electrical Engineering and Telecommunications, The University of New South Wales, Sydney, Australia. He also has a number of years of industrial experience in senior positions, in both start-ups and multinational companies, including Toucan Technology Ltd., PMC-Sierra Inc., Innovada Ltd., and Duolog Technologies Ltd. He also represented Toucan Technology and PMC-Sierra on international standardization groups ANSI T1E1.4 and ETSI TM6. His current research interests include DSP algorithm development and embedded implementation for applications in biomedical engineering, speech and audio processing, and image processing. He is also a Chartered Engineer and a fellow of the Institution of Engineers of Ireland.

MARTIN GLAVIN (Member, IEEE) received the B.E. degree in electronic engineering and the Ph.D. degree in algorithms and architectures for high-speed data communications systems from the University of Galway, Ireland, in 1997 and 2004, respectively, and the Diploma degree in third level education, in 2007. He was a Lecturer (fixed term contract), from September 1999 to December 2003, and became a permanent member of the Academic Staff, in January 2004. He is currently the Joint Director of the Connaught Automotive Research (CAR) Group, University of Galway. He is also a Funded Investigator with the Irish Software Research Centre, Lero. He has a number of Ph.D. students and postdoctoral researchers working in collaboration with industry in the areas of signal processing and embedded systems for automotive and agricultural applications.

BRIAN DEEGAN received the bachelor's degree in computer engineering and the M.Sc. degree in biomedical engineering from the University of Limerick, in 2004 and 2005, respectively, and the Ph.D. degree in biomedical engineering from the University of Galway, in 2011. The focus of his research was the relationship between blood pressure and cerebral blood flow in humans. From 2011 to 2022, he was with Valeo Vision Systems as a Vision Research Engineer focusing on image quality. His research interests include high dynamic range imaging, LED flicker, top view harmonization algorithms, and the relationship between image quality and machine vision. In 2022, he joined the Department of Electrical and Electronic Engineering, University of Galway, as a Lecturer and a Researcher.